Effect of Molecular Configuration on Binary Diffusion Coefficients of Linear Alkanes

Kyungchan Chae, Paolo Elvati, and Angela Violi*

Department of Mechanical Engineering, The University of Michigan, Ann Arbor, Michigan, 48109-2125

Received: September 21, 2010; Revised Manuscript Received: November 15, 2010

Mass diffusion coefficients are critically related to the predictive capability of computational combustion modeling. To date, the most common approach used to determine the molecular transport of gases is the Boltzmann transport equation of the gas kinetic theory. The Chapman−Enskog (CE) solution of this transport equation, combined with Lennard-Jones potential parameters, suggests a simple analytical expression for computing self and mutual diffusion coefficients. This approach has been applied over a wide range of flame modeling conditions due to its minimal computational requirement, despite the fact that the theory was developed only for molecules that have a spherical structure. In this study, we computed the binary diffusion coefficients of linear alkanes using all-atom molecular dynamics simulations over the temperature range 500−1000 K. The effect of molecular configurations on diffusion coefficients was determined relating the radii of gyration of the molecules to their corresponding collision diameters. The comparison between diffusion coefficients determined with molecular dynamics and the values obtained from the CE theory shows significant discrepancies, especially for nonspherical molecules. This study reveals the inability of CE theory with spherical potentials to account for the effect of molecular shapes on diffusion coefficients.

1. Introduction

Combustion modeling is an essential tool for the prediction of flame characteristics as well as for the optimal design of combustors. Mass diffusion coefficients and chemical kinetic mechanisms are essential input data to investigate complex flame behaviors, such as flame speed, heat and mass transfer, and ignition characteristics. Although, chemical kinetic mechanisms of hydrocarbons have been widely studied,[1−3] molecular transport data of those species, especially for molecules with a large number of atoms, have not yet experienced similar focus.[4−6]

Over the years, kinetic theory for polyatomic gases has been formulated in three different ways. Taxman suggested the classical kinetic theory.[7] Wang Chang and Uhlenbeck developed the semiclassical theory, which describes internal quantum states of a molecule as separate chemical species, and treats translational motion classically.[8] Waldmann[9] and Snider[10] derived a fully quantum mechanical kinetic theory. Direct application of these theories to polyatomic molecules, however, is still hindered by difficulties in assessing the dynamics of molecular collisions. Therefore, the analysis of collision dynamics must rely on approximations of collision integrals, which account for interaction energy related to intermolecular pair potentials, as well as the scattering mechanism of molecular collisions.[11]

The most widely used approximation scheme for evaluating angular dependent interactions for transport properties has been proposed by Monchick and Mason.[12] Their approach reduces the mathematical model of collisions to computationally manageable equations. The collision integrals for a given pair of molecules are tabulated as a function of the reduced temperature, $T^* = k_B T/\varepsilon_{12}$, where ε_{12} is the energy well depth of the intermolecular potentials between two molecules, and k_B is the Boltzmann constant.

The Chapman−Enskog solution of the Boltzmann transport equation (CE) produces a simple mathematical expression for mutual diffusion coefficients.[7] Hirschfelder et al. followed the Chapman−Enskog approach, combined with the Lennard-Jones (LJ) 12-6 intermolecular potential function, and suggested the Hirschfelder−Bird−Spotz (HBS) equation for mutual mass diffusion coefficients[13]

$$D_{12} = \frac{3}{8}\frac{\sqrt{(k_B T)^3/(2\pi m_{12})}}{n\sigma_{12}^2\langle\Omega^{(1,1)^*}\rangle} \quad (1)$$

T is the temperature of the system, m_{12} is the reduced mass of the pair components, n is the average number density, σ_{12} is the collision diameter of two species, and $(\Omega^{(1,1)^*})$ is the collision integral and it depends on the reduced temperature. The main disadvantage of this equation is the difficulty encountered in evaluating the collision diameter, σ_{12}, and potential energy well depth, ε_{12}. These two parameters are usually obtained from viscosity measurements.[13] However, only a limited amount of data is available for polyatomic molecules. Therefore, the correlations of corresponding states of Tee et al. are frequently employed to estimate the parameters for fluids.[14]

The validity of eq 1 is limited to low density gases with the assumption of spherical interactions between molecules. Despite these limitations, eq 1 has been extensively employed to determine transport properties of significant nonspherical molecules in high temperature conditions.

Recent investigations have reported the importance of mass diffusion coefficients in flame modeling.[15−18] H_2/air flame simulations showed up to 30% difference in extinction strain rate when different transport formulations were employed.[15] Modeling of nonpremixed flames of hydrocarbons have highlighted the importance of the size and mobility of molecules on the extinction strain rates; as the size of molecules decreases, resistance to extinction strain rate increases.[17] Sensitivity analyses of ignition, laminar flame speed, and extinction strain rates have reported that the sensitivity of diffusion could be on the same order or larger than chemical kinetics.[15,16,18]

* To whom correspondence should be addressed. E-mail: avioli@umich.edu.

10.1021/jp109042q
Published on Web 12/15/2010

In this paper, we compute the diffusion coefficients of linear hydrocarbons using all-atom molecular dynamics (MD) simulations and we propose possible modifications to the HBS equation to improve the prediction of diffusion coefficients for molecules with nonspherical symmetry. One of the main goals of this study is to identify and quantify the effect of molecular structure on diffusion. All-atom molecular dynamics simulations are employed to overcome the limitations of the CE theory with spherical potentials and provide an explicit way to compute diffusion coefficients of polyatomic molecules.

As systems of interest, we focused on linear alkanes, since they are the most abundant constituents of conventional hydrocarbon fuels. We selected 16 linear alkanes (from methane, CH_4, to hexadecane, $C_{16}H_{34}$) to assess the effect of the length of the molecular chain on diffusion coefficients.

After describing the methodology used for the molecular dynamics simulations, we report on the computed diffusion coefficients of hydrocarbons in the temperature range 500−1000 K and compare the results with the values obtained using the HBS equation. The main discrepancies are identified for nonspherical molecules, suggesting the need for a correction factor when using the HBS approach. In the last section of the paper, we recommend a new expression of the collision diameters that takes into account the radius of gyration to include the effect of molecular configurations on the diffusion coefficients.

2. Methodology

One of the methods to determine the transport properties from molecular dynamics simulations is based on the fluctuation dissipation theorem and the Green−Kubo (GK) formula.[19−21] The GK formula expresses the self-diffusion coefficient as the ensemble average of the velocity autocorrelation functions of time. The binary mass diffusion coefficient is defined as the combination of the ensemble average of velocity auto- and cross-correlation functions of time.[22] The binary diffusion coefficient is[23]

$$D_{12} = Q\left[x_2 D_1 + x_1 D_2 + x_1 x_2 \left(\frac{f_{11}}{x_1^2} + \frac{f_{22}}{x_2^2} - 2\frac{f_{12}}{x_1 x_2}\right)\right] \quad (2)$$

$$D_\alpha = \frac{1}{3}\int_0^\infty \langle \vec{u}_i^\alpha(t)\cdot\vec{u}_i^\alpha(0)\rangle \, \mathrm{d}t \quad (3)$$

$$f_{\alpha\alpha} = \frac{1}{3}\int_0^\infty \langle \vec{u}_i^\alpha(t)\cdot\vec{u}_j^\alpha(0)\rangle \, \mathrm{d}t \quad (4)$$

$$f_{\alpha\beta} = \frac{1}{3}\int_0^\infty \langle \vec{u}^\alpha(t)\cdot\vec{u}^\beta(0)\rangle \, \mathrm{d}t \quad (5)$$

where D_α is the time integral of velocity autocorrelation functions of species α; $\vec{u}^\alpha$ and $\vec{u}^\beta$ are velocity vectors of species α and β; and $f_{\alpha\alpha}$ and $f_{\alpha\beta}$ are the time integrals of the velocity cross-correlation function between the same species and between species α and β, respectively. x_α is the mole fraction of each species, while the angular brackets denote the ensemble average.[24] The Q factor can be determined from the integral of the radial distribution functions. For a binary mixture system, the parameter Q is defined as[23]

$$Q = \frac{1}{1 + x_1 x_2 \rho(\Gamma_{11} + \Gamma_{22} - 2\Gamma_{12})} \quad (6)$$

$$\Gamma_{\alpha\alpha} = 4\pi\int_0^\infty r^2[g_{\alpha\alpha}(r) - 1]\,\mathrm{d}r \quad (7)$$

$$\Gamma_{\alpha\beta} = 4\pi\int_0^\infty r^2[g_{\alpha\beta}(r) - 1]\,\mathrm{d}r \quad (8)$$

where $g_{\alpha\alpha}(r)$ and $g_{\alpha\beta}(r)$ are the radial distribution functions between the same species and between species α and β, respectively. $\Gamma_{\alpha\alpha}$ and $\Gamma_{\alpha\beta}$ represent the spatial integrals of the radial distribution functions. For a thermodynamically ideal mixture, defined as the perfectly mixed state of a mixture, the integrals of the radial distribution functions of each species are identical, and Q can be approximated as unity.[25]

2.1. Force Field. The OPLS AA force field, used in this study, is an empirical all atom force field that has been applied to a wide range of hydrocarbon molecules.[26] This force field has been employed to obtain thermodynamic and transport properties of various systems that consist of polyatomic molecules, and the results of these studies showed good agreement with available experimental data.[27−31]

The OPLS AA force field utilizes the Lennard-Jones (L-J) 12-6 potential model for determining intermolecular interactions. A cutoff distance of 18 Å was used for these interactions as well as for the electrostatic potential. All molecules were treated as fully flexible, allowing bond stretching and angle vibration, as well as the change of torsion angles.

2.2. Systems of Interest. Simulations were conducted in the temperature range 500−1000 K at 1 atm. For each mixture, the results of five simulations were averaged in order to increase the statistical accuracy of velocity correlations. The total simulation time was 14 ns, and velocity components of each atom were recorded every 50 time steps. The leapfrog algorithm was used with a time step of 1.0 fs to integrate the equation of motion. All MD simulations were carried out with the GROMACS software package.[32]

In defining system sizes, we used experimentally measured densities at each temperature and utilized cubic periodic boundary conditions. The canonical ensemble (NVT) was obtained by employing a global Nose−Hoover thermostat with a time constant of 100 ps.[33,34]

3. Results

As a first step, we evaluated the accuracy of our choice of the NVT ensemble for the simulations. The Nose−Hoover thermostat controls the temperature of the system by expanding phase space with scaled momentum,[35] and the velocity components of particles are perturbed by this scaling method. Therefore, computing transport properties requires a very weak perturbation so that the thermostat exerts a negligible influence on the final results. Previous studies of self and binary diffusion coefficients of N_2, CO_2, C_2H_6, and C_2H_4 showed that the Nose−Hoover global thermostat does not modify the diffusion coefficient in a significant way.[36] To verify the applicability of NVT simulations, we computed the velocity autocorrelation functions obtained using the NVE and NVT ensembles for normal heptane and nitrogen (n-C_7H_{16}/N_2) mixtures at two different temperatures (500 and 1000 K). As shown in Figure 1, the velocity autocorrelation functions are well matched. We also compared the diffusion values computed with different time constants in the range 1.0−100.0 ps, and the difference was

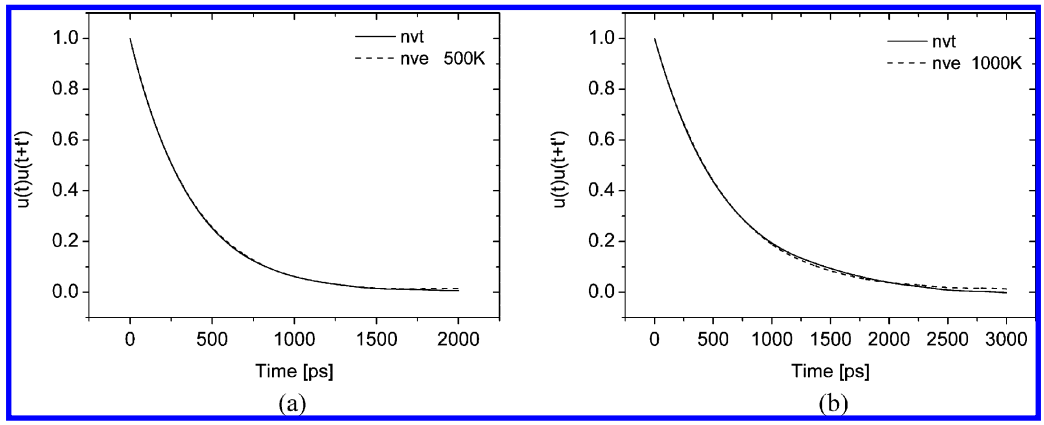

Figure 1. Velocity autocorrelation functions of n-C_7H_{16} with NVE and NVT (1.0 ps coupling parameter) ensembles at 1 atm and (a) 500 K and (b) 1000 K.

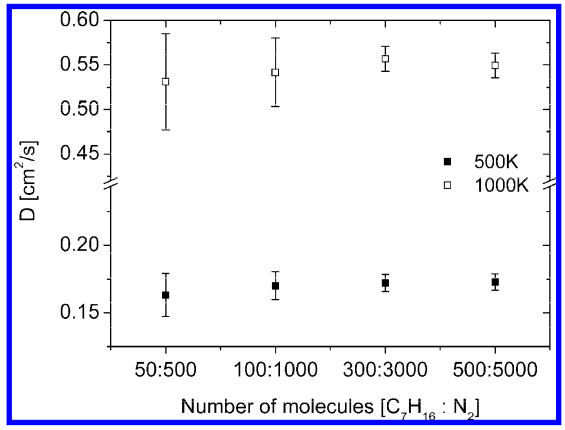

Figure 2. Mutual diffusion coefficients of n-C_7H_{16}/N_2 mixtures at 1 atm for different system sizes, obtained from MD simulations.

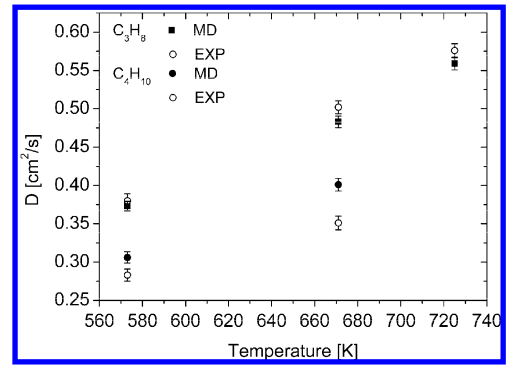

Figure 3. Mutual diffusion coefficients of n-C_3H_8/N_2 and n-C_4H_{10}/N_2 mixtures at 1 atm (MD, molecular dynamics simulations; EXP, experiment).

less than 1% irrespective of the applied coupling parameters. These results can be explained considering the high temperature and low density of the systems under investigation. On the basis of these results, we concluded that for our systems the global Nose−Hoover thermostat has a negligible effect on the diffusion coefficients and therefore we can safely employ it in our study.

Figure 1 also shows that the velocity is sufficiently decorrelated within 3 ns even at low temperature. In the calculations reported in the next sections, we used a longer sampling time (7 ns) to improve the statistical accuracy in the tail region.

To test the effect of the size of the system (number of atoms in the computational box) on diffusion coefficients, we simulated four different systems composed of n-C_7H_{16}/N_2. The results reported in Figure 2 show that the diffusion coefficients for the four systems are very similar. However, system B (1100 molecules) has a much larger statistical error than systems C (3300 molecules) and D (5500 molecules), especially at high temperature (1000 K). Although increasing the size of the system will slowly but steadily reduce the error, we used systems composed of 3300 molecules for our simulations as a compromise between accuracy and computational costs.

The concentration of alkanes was set at 10% in our simulations because of our interest in studying real combustion systems. To observe the effect of the relative concentration of species on mutual diffusion coefficients, we varied the concentration of n-C_7H_{16} between 1 and 10% in nitrogen and the variation in the computed mutual diffusion coefficients was around 1%. This result is expected due to the weak dependency of diffusion coefficients on concentration in the limit of low density, weakly interacting gas mixtures.

Since the OPLS AA potential parameters were optimized at normal boiling temperature, direct application of this force field to different temperature conditions cannot guarantee the accuracy of computed diffusion coefficients. Therefore, we compared our MD results with available experimental data to identify the validity of the potential under such conditions. As reported in Figure 3, simulations of n-C_3H_8/N_2 mixtures show a better agreement with experimental results (3% deviation) than n-C_4H_{10}/N_2 mixtures (10% deviation). It is worth noting that the results for n-C_3H_8/N_2 were obtained recently using the reverse-flow gas chromatographic technique,[37] while the systems of n-C_4H_{10}/N_2 mixtures were studied around 30 years ago.[38] Nevertheless, when considering the uncertainty of the experimental measurements (around 3%),[37] we concluded that MD results are in reasonably good agreement with experimental data. Consequently, we believe that the OPLS AA force field can produce reliable diffusion coefficients for the high temperature regime used in this study.

3.1. Diffusion Coefficients and Temperature Effect of *n*-Alkanes. In a recent publication, we verified the ability of MD simulations to capture the effect of molecular structure on diffusion coefficients investigating systems composed of molecules with the same mass but different shapes, such as heptane isomers.[39] In this study, we extend the previous work and we look at systems composed of molecules with the same configurations but different masses. MD results for the binary diffusion coefficients of alkanes from methane, CH_4, to hexadecane, $C_{16}H_{34}$, are presented in Figure 4. As the number of methyl groups increases, the diffusion coefficients decrease. Moreover, the difference in diffusion coefficients among mixtures becomes larger as the temperature increases. Experimental measurements of mutual diffusion coefficients for gas mixtures at 1 atm showed

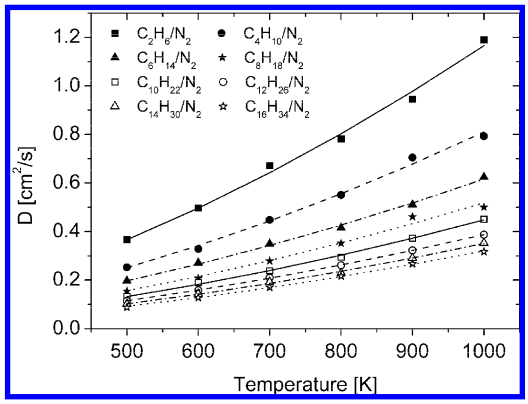

Figure 4. Mutual diffusion coefficients of linear alkanes in nitrogen as a function of temperature, obtained from MD simulations. The curves correspond to the power function curve fitting of diffusion coefficients.

that the temperature dependence can be written in the following form:[37,40]

$$D_{12} = AT^n \tag{9}$$

where A and n are fitting constants and T is the temperature of the system. The above equation successfully describes also the temperature dependency of computed diffusion coefficients. Detailed results for all linear alkanes are listed in Table S.1 in the Supporting Information.

The HBS equation (eq 1) is advantageous in computing mutual diffusion coefficients due to its simplicity. However, the lack of potential parameters (collision diameter, σ, and energy well depth, ε) for molecules significantly limits its application. These potential parameters, especially for polyatomic molecules, are rarely available. Therefore, in this study, we employed correlations of the corresponding state theory of Tee et al. to estimate potential parameters.[14] Critical temperature (T_c) and pressure (P_c) and normal boiling temperature (T_b) were obtained from the NIST chemistry web database. Table S.2 in the Supporting Information lists the thermodynamic parameters and computed potential parameters (σ and ε) for the hydrocarbons considered in this study.

Figure 5 reports the diffusion coefficients for four mixtures of hydrocarbons in nitrogen obtained using MD simulations and the HBS equation. This comparison is meant to demonstrate that the deviation in diffusion values originates from the utilization of monatomic spherical potentials. For the C_2H_6/N_2 mixture, the agreement between MD simulations and HBS values is good. The same comparison carried out for the $C_{16}H_{34}/N_2$ mixture shows significant differences between the two methods. The average deviation is around 17%, with MD underestimating the diffusion values compared with the HBS equation. The overall results in Figure 6 suggest that the HBS approach produces values of the diffusion coefficients similar to MD when the molecules have spherical symmetry, i.e., CH_4 or C_2H_6. In other words, using single body interaction potentials is not appropriate for molecules that have nonspherical structures.

In order to quantify the difference in diffusion values between the two approaches, we searched for a geometric factor that could represent the molecular structures obtained from MD simulations and at the same time could be compared with a collision diameter (σ). For this purpose, we computed the radius of gyration (R_g) of each hydrocarbon molecule from MD simulations using the following relation:

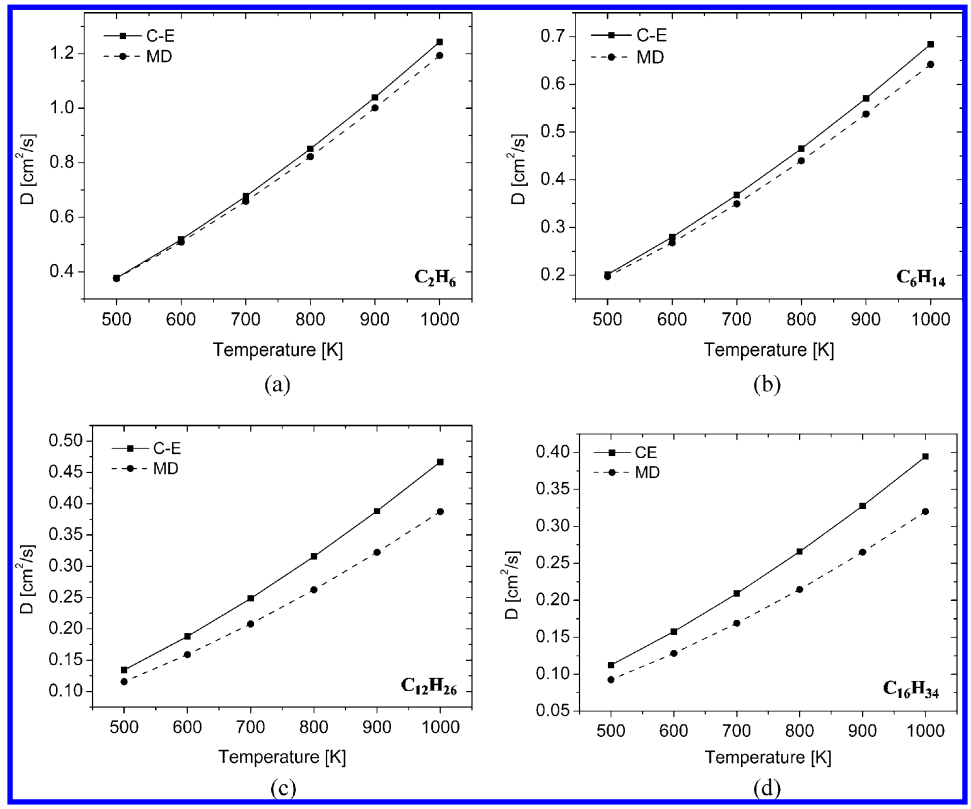

Figure 5. Mutual diffusion coefficients of (a) C_2H_6/N_2, (b) C_6H_{14}/N_2, (c) $C_{12}H_{26}/N_2$, and (d) $C_{16}H_{34}/N_2$ at 1 atm (MD, molecular dynamics; CE, HBS equation). The curves correspond to the power function curve fitting of diffusion coefficients.

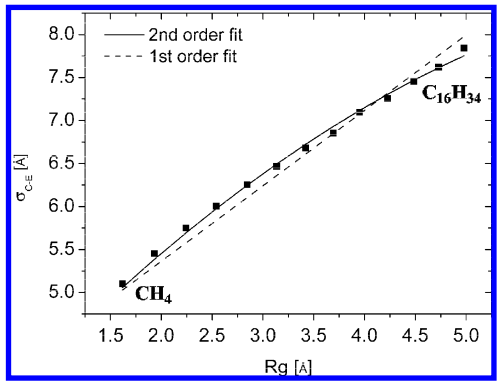

Figure 6. Collision diameters (σ_{CE}) of linear alkanes obtained from CE results and relations with average radius of gyrations (R_g).

TABLE 1: Contributions of Collision Diameter σ and Energy Well Depth ε to the Diffusion Coefficients of the n-C_7H_{16}/N_2 Mixture When 10% Perturbation Is Exerted

	D_{12} (cm^2/s)		
temperature (K)	no perturbation	perturbed σ	perturbed ε
500	0.185	0.164	0.182
1000	0.630	0.559	0.623
deviation(%)	0	11.3	1.5

$$R_g = \sum_{\alpha=1}^{3} I_{\alpha\alpha} \tag{10}$$

where $I_{\alpha\alpha}$ denotes the moments of inertia of principal axes.

An important difference between σ and R_g is the temperature dependence of the latter, which makes the analysis of the diffusion trends complex. However, the computed values of R_g in the temperature range 500−1000 K did not vary significantly. Table S.3 in the Supporting Information lists the average radii of gyration of the linear alkanes computed from MD simulations.

In Figure 6, we plot the collision diameters of linear alkanes used in eq 1 (σ_{CE}) (Table S.2 in the Supporting Information) versus the average radii of gyration (Table S.3 in the Supporting Information). As the length of the chain of alkanes increases, the radii of gyration and collision diameters also increase. The similarity depicted in the figure demonstrates that R_g is related to σ, as expected since both characterize the molecular size, yet the radius of gyration imbeds geometric factors that are not captured by the collision diameter of a spherical potential function. The CE theory can be used to compute diffusion coefficients of nonspherical polyatomic molecules only when the collision diameters (σ_{CE}) are linearly related to the radii of gyration (R_g). The second order fitting curve represents the deviation from sphericity of the molecules (Figure 6).

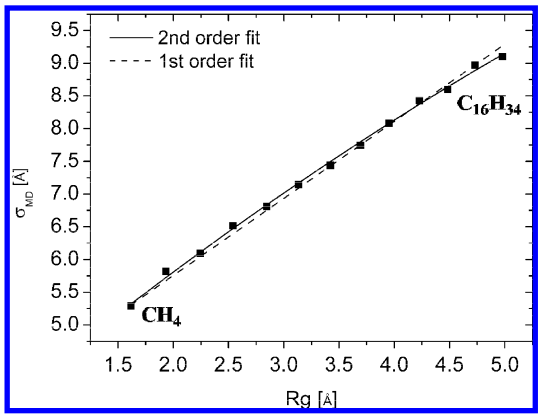

Figure 7. New collision diameters of linear alkanes obtained from MD versus the average radii of gyrations (R_g).

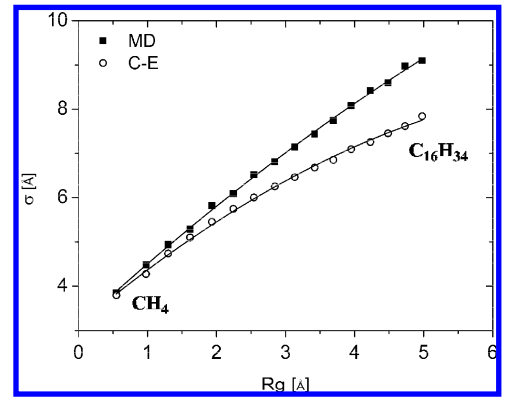

Figure 8. Collision diameters of linear alkanes obtained from MD and CE equation versus the radii of gyration. Each point in the series corresponds to an alkane, from methane with $R_g = 0.5$ to hexadecane with $R_g = 5$. Curves represent second-order fitting of σ_{MD} and σ_{CE}, respectively.

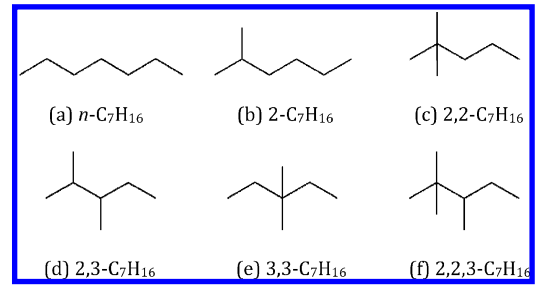

Figure 9. Molecular configurations of heptane isomers.

Using the values of diffusion coefficients from MD simulations, we determined new collision diameters (σ_{MD}) from eq 1 for the hydrocarbon molecules. For the energy well depth (ε), we used the same values employed in the HBS equation (Table S.2 in the Supporting Information), since the inverse square of σ is proportional to diffusion coefficients. As shown in Table 1, 10% perturbation of σ causes around 11.3% deviation from the original diffusion values. On the other hand, the same amount of perturbation of ε produces only 1.5% deviation. This result confirms that σ has a dominant effect on determining diffusion values when compared with the energy well depths.

Figure 7 reports the first and second order fitting curves of σ_{MD} versus R_g, showing only a small deviation from linearity, that likely results from the temperature dependence of the radius of gyration and the effect of energy well depths.

The comparison between σ_{MD} and σ_{CE} for linear alkanes in Figure 8 shows that the HBS equation produces larger deviations as the number of methyl groups in the chain increases, raising concerns regarding the ability of the CE theory coupled with spherical potentials to produce reliable diffusion coefficients for polyatomic molecules.

The relation between σ_{MD} and σ_{CE} for linear alkanes is obtained combining the two second order fitting expressions, and it is reported in eq 11. The dependence on R_g represents a simple way to take into account the effect of molecular configurations when using the CE theory with spherical potentials.

$$\sigma_{MD} = \frac{3.1 + 1.4R_g - 4.6E - 2R_g^2}{3.1 + 1.3 - 7.8E - 2R_g^2}\sigma_{CE} \tag{11}$$

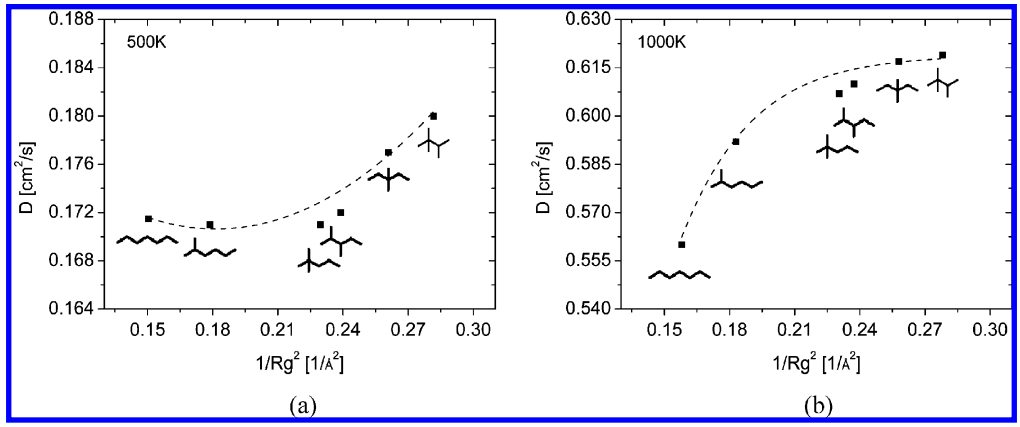

Figure 10. Mutual diffusion coefficients of heptane isomers in nitrogen versus the inverse of the squared radius of gyrations (R_g) of the isomers at (a) 500 K and (b) 1000 K. The curves are from reference 39.

3.2. Linear Alkanes with Methyl Branches. In this section, we apply our computational approach to systems composed of heptane isomers in nitrogen to assess the effect of molecular shape on diffusion coefficients. Since all isomers have the same mass, deviations in computed diffusion coefficients originate entirely from the arrangement of methyl branches. Figure 9 shows the molecular configurations of the six heptane isomers considered in this analysis.

In Figure 10, we report the diffusion coefficients of the isomers versus their corresponding radii of gyration. As the radius of gyration of the isomer decreases, the values of the diffusion coefficients increase, which is consistent with the fact that, in gas kinetic theory, smaller collision diameters produce larger diffusion coefficients. The relative location of methyl branches influences the collision diameters (and R_g). Among the three isomers that have the same number of methyl branches (2,2-C_7H_{16}, 2,3-C_7H_{16}, and 3,3-C_7H_{16}), 3,3-C_7H_{16} has the smallest R_g value and 2,2-C_7H_{16} has the largest R_g value. This result shows that, when methyl branches are close to the center of the molecules, R_g becomes smaller and therefore the diffusion coefficient increases.

4. Conclusions

In this study, we computed the binary diffusion coefficients of 16 linear alkanes in nitrogen using both the Chapman−Enskog (CE) theory with spherical potentials (HBS equation) and molecular dynamics simulations. Our primary interest was to determine the diffusion coefficients of polyatomic molecules with nonspherical geometries and assess the effect of molecular structure on transport properties. After comparing the results from MD with the ones from HBS for various hydrocarbons in the temperature range 500−1000 K, we employed the radius of gyration to quantify the effect of molecular configurations on diffusion coefficients. The radii of gyration obtained from MD simulations were correlated with the collision diameters used in the HBS equation, showing that for polyatomic molecules with nonspherical geometries the HBS equation needs to be corrected using the radius of gyration. A new expression for the collision diameters for linear alkanes is also presented.

The radius of gyration can be used also to determine accurate values of the diffusion coefficients of alkane isomers. To this end, we investigated systems composed of heptane isomers in nitrogen. As for linear alkanes, the radius of gyration can successfully explain the trends of diffusion coefficients, showing that methyl branches reduce the collision diameters and lead to larger diffusion coefficients than linear alkanes, as reported experimentally.

Acknowledgment. This research is funded by the U.S. Air Force Office of Scientific Research (Grant F022058) under the technical supervision of Dr. Julian M. Tishkoff.

Supporting Information Available: Tables showing diffusion coefficients for all of the alkanes in the temperature range, thermodynamic properties and potential parameters (σ_{CE} and ε), and radii of gyration of the different alkanes. This material is available free of charge via the Internet at http://pubs.acs.org.

References and Notes

(1) Ingemarsson, A. T.; Pedersen, J. R.; Olsson, J. O. *J. Phys. Chem. A* **1999**, *103*, 8222.
(2) Zhang, H. R.; Eddings, E. G.; Sarofim, A. F.; Westbrook, C. K. *Energy Fuels* **2007**, *21*, 1967.
(3) Calemma, V.; Peratello, S.; Stroppa, F.; Giardino, R.; Perego, C. *Ind. Eng. Chem. Res.* **2004**, *43*, 934.
(4) Ern, A.; Giovangigli, V. *Combust. Sci. Technol.* **1999**, *149*, 157.
(5) Williams, B. A. *Combust. Flame* **2001**, *124*, 330.
(6) Middha, P.; Yang, B. H.; Wang, H. *Proc. Combust. Inst.* **2002**, *29*, 1361.
(7) Taxman, N. *Phys. Rev.* **1958**, *110*, 1235.
(8) Wang Chang, C. S.; Uhlenbeck, G. E. Michigan University Engineering Research Institute Report 1951, CM.
(9) Waldmann, L. *Z. Naturforsch., A: Astrophys., Phys. Phys. Chem.* **1957**, *12*, 660.
(10) Snider, R. F. *J. Chem. Phys.* **1960**, *32*, 1051.
(11) Millat, J.; Dymond, J. H.; Castro, C. A. N. d. *Transport Properties of Fluids: Their correlation, prediction and estimation*; Cambridge University Press: Cambridge, 1996.
(12) Monchick, L.; Mason, E. A. *J. Chem. Phys.* **1961**, *35*, 1676.
(13) Reid, R. C.; Prausnitz, J. M.; Poling, B. E. *The Properties of Gases and Liquids*, 4th ed.; McGraw-Hill: New York, 1987.
(14) Tee, L. S.; Gotoh, S.; Stewart, W. E. *Ind. Eng. Chem. Fundam.* **1966**, *5*, 356.
(15) Dong, Y. F.; Holley, A. T.; Andac, M. G.; Egolfopouos, F. N.; Davis, S. G.; Middha, P.; Wang, H. *Combust. Flame* **2005**, *142*, 374.
(16) Holley, A. T.; Dong, Y.; Andac, M. G.; Egolfopoulos, F. N. *Combust. Flame* **2006**, *144*, 448.
(17) Holley, A. T.; Dong, Y.; Andac, M. G.; Egolfopoulos, F. N.; Edwards, T. *Proc. Combust. Inst.* **2007**, *31*, 1205.
(18) Holley, A. T.; You, X. Q.; Dames, E.; Wang, H.; Egolfopoulos, F. N. *Proc. Combust. Inst.* **2009**, *32*, 1157.
(19) Kubo, R. *J. Phys. Soc. Jpn.* **1957**, *12*, 570.
(20) Kubo, R.; Yokota, M.; Nakajima, S. *J. Phys. Soc. Jpn.* **1957**, *12*, 1203.
(21) Zwanzig, R. *Annu. Rev. Phys. Chem.* **1965**, *16*, 67.
(22) Sharma, R.; Tankeshwar, K. *J. Chem. Phys.* **1998**, *108*, 2601.
(23) Zhou, Y. H.; Miller, G. H. *J. Phys. Chem.* **1996**, *100*, 5516.
(24) Olivet, A.; Vega, L. F. *J. Phys. Chem. C* **2007**, *111*, 16013.
(25) Stoker, J. M.; Rowley, R. L. *J. Chem. Phys.* **1989**, *91*, 3670.
(26) Jorgensen, W. L.; Maxwell, D. S.; TiradoRives, J. *J. Am. Chem. Soc.* **1996**, *118*, 11225.
(27) Petravic, J.; Delhommelle, J. *Chem. Phys.* **2003**, *286*, 303.
(28) Zhang, L.; Wang, Q.; Liu, Y. C.; Zhang, L. Z. *J. Chem. Phys.* **2006**, *125*, 104502.

(29) Yang, Q. Y.; Xue, C. Y.; Zhong, C. L.; Chen, J. F. *AIChE J.* **2007**, *53*, 2832.

(30) Price, M. L. P.; Ostrovsky, D.; Jorgensen, W. L. *J. Comput. Chem.* **2001**, *22*, 1340.

(31) Thomas, L. L.; Christakis, T. J.; Jorgensen, W. L. *J. Phys. Chem. B* **2006**, *110*, 21198.

(32) Lindahl, E.; Hess, B.; van der Spoel, D. *J. Mol. Model.* **2001**, *7*, 306.

(33) Nose, S. *J. Chem. Phys.* **1984**, *81*, 511.

(34) Hoover, W. G. *Phys. Rev. A* **1985**, *31*, 1695.

(35) Frenkel, D.; Smit, B. *Understanding molecular simulation; from algorithms to applications*; Academic Press: San Diego, 1996.

(36) Fernandez, G.; Vrabec, J.; Hasse, H. *Int. J. Thermophys.* **2005**, *26*, 1389.

(37) Manion, J. A.; McGivern, W. S. Combustion Institute 2008 spring technical meeting, Western states sections 2008.

(38) Wakeham, W. A.; Slater, D. H. *J. Phys. B: At., Mol. Opt. Phys.* **1973**, *6*, 886.

(39) Chae, K.; Violi, A. *J. Chem. Phys.*, in press.

(40) Manion, J. A.; McGivern, W. S. 6th US national combustion meeting 2009.

JP109042Q